Synthesis and Reversible H2 Activation by Coordinatively Unsaturated Rhodium NHC Complexes

Author(s):
Lutz, Marius (iD); Zhong, Hongyu (iD); Trapp, Nils; Morandi, Bill

RESEARCH ARTICLE

HELVETICA

Synthesis and Reversible H$_2$ Activation by Coordinatively Unsaturated Rhodium NHC Complexes

Marius D. R. Lutz,[a] Hongyu Zhong,[a] Nils Trapp,[a] and Bill Morandi*[a]

[a] Laboratorium für Organische Chemie, ETH Zürich, CH-8093 Zürich, Switzerland,
e-mail: bill.morandi@org.chem.ethz.ch

In memory of Professor *Jack D. Dunitz*

We report the synthesis of coordinatively unsaturated cationic rhodium complexes bearing the sterically encumbered electron-rich NHC ligand IPr*^{OMe}. The COD (1,5-cyclooctadiene) complex [Rh(IPr*^{OMe})(COD)]BF$_4$ adopts a tilted, pseudo-square planar coordination geometry, where bonding to the *ipso*-carbon of the NHC aryl substituent was observed in the solid state. Hydrogenation of this complex afforded a metastable dihydride complex [Rh(IPr*^{OMe})(H)$_2$]BF$_4$ with an unusual internal coordination to an arene of the ligand. In the absence of a hydrogen atmosphere, spontaneous reductive elimination of H$_2$ afforded a rhodium complex [Rh(IPr*^{OMe})]BF$_4$ with a single chelating ligand that stabilizes the highly unsaturated metal by two-fold π-face donation as suggested by NMR spectroscopy and computational studies. This unusual complex might serve as a versatile precatalyst for a variety of transformations.

Keywords: coordinative unsaturation, crystallography, hydrogenation, *N*-heterocyclic carbenes, reversible H$_2$ activation, rhodium.

Introduction

Achieving coordinative unsaturation is central to transition metal catalysis because substrate coordination and subsequent bond-breaking and -forming events require empty coordination sites on the metal. An important advantage of monodentate ligands compared to bidentate ligands is the possibility to achieve a higher degree of coordinative unsaturation with a metal. The resulting complexes are then more susceptible towards substrate coordination and following oxidative addition.[1] A notable example of this is the *Buchwald* mono(phosphine) ligand family which has gained tremendous success in Pd-catalyzed C–C and C–N bond coupling reactions (*Figure 1,a*).[1] A key design element is the bi-aryl substituent on the phosphine, where weak coordination through the
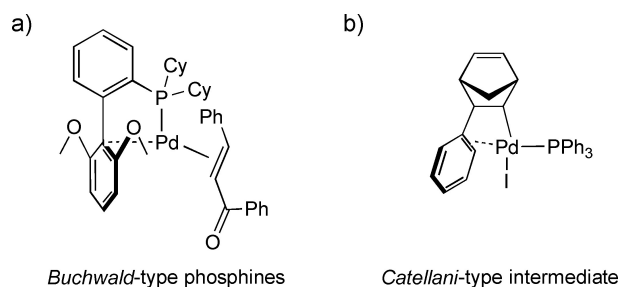
Figure 1. Selected examples of coordinatively unsaturated metal complexes featuring weak interactions with the ligand.

ipso-carbon to Pd(0) endows this ligand with a hemi-labile character to transiently stabilize on-cycle species by going from a 14 e$^-$ to a 16 e$^-$ configuration.[2] Similar stabilization through *ipso*-carbon coordination has also been observed in the Pd(II) norbornyl intermediates relevant in the *Catellani* reaction (*Figure 1,b*).[3,4]

Supporting information for this article is available on the WWW under https://doi.org/10.1002/hlca.202200199

Another class of monodentate ligands, *N*-heterocyclic carbenes (NHC), and related cyclic(alkyl)(amino)-carbenes (CAAC), have also found widespread applications in transition metal catalysis.[5–11] For example, palladium NHC catalysts are highly active in challenging *Buchwald–Hartwig* amination reactions.[5,8,12–15] Further, rhodium NHC complexes are active catalysts in the reversible formation of strong C—C bonds[16–19] and arene hydrogenations.[20–26] It has been found that in many cases cationic group 9 complexes are more active hydrogenation catalysts compared to their fully coordinated neutral analogs, a prominent example being *Crabtree*'s catalyst.[27–31] Among the reported (NHC)Rh(I)(COD) and (NHC)Ir(I)(COD) complexes bearing a cationic metal center, a second dative interaction from the NHC ligand in addition to the carbene coordination leads to a metal with a formal 16 e$^-$ configuration (*Figure 2*).[32–40] However, unfavorable ligand dissociation can become prominent under harsher reaction conditions (*e.g.*, high hydrogen pressure), leading to irreversible ligand decoordination and nanoparticle generation. For example, rhodium nanoparticles have been found to be the active catalyst in an originally thought-to-be homogeneous (CAAC)rhodium-catalyzed arene hydrogenation.[20,22,26] The formation of not well-defined nanoparticles can cause reproducibility problems and render a mechanistic investigation challenging.[41]

To arrive at a coordinatively unsaturated rhodium NHC complex that also remains stable towards decomposition, we reasoned that a sterically encumbered NHC ligand with peripheral aryl groups might be ideal.
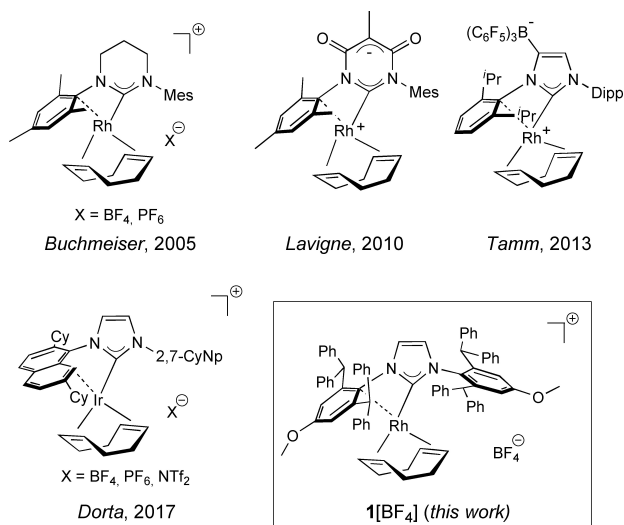
We therefore investigated the synthesis and reactivity of the coordinatively unsaturated complex [Rh-(IPr*^{OMe})(COD)]BF$_4$ (**1**[BF$_4$]), a cationic version of the active complex we recently used in reversible shuttle arylation catalysis, towards hydrogen.[42] Facile hydrogenation of the COD ligand in **1**[BF$_4$] under mild conditions afforded a characterizable Rh(III) dihydride complex with internal η^6-coordination to one phenyl group on the ligand. This dihydride complex reversibly reductively eliminates H$_2$ and the resulting Rh(I) center coordinates to two phenyl substituents on the NHC ligand, as supported by ^{1}H-, ^{13}C{^{1}H}-, and ^{103}Rh-NMR spectroscopy as well as density functional theory (DFT) computations.

Results and Discussion

Synthesis and X-Ray Structure of Tilted NHC Rhodium Complex **1**[BF$_4$]

Cationic complex **1**[BF$_4$] was synthesized by salt metathesis from [Rh(IPr*^{OMe})(COD)Cl].[42] Addition of AgBF$_4$ to a THF solution of the chloride complex, followed by filtration and precipitation afforded pure **1**[BF$_4$] in 82 % yield (*Scheme 1*). The single-crystal X-ray structure of complex **1**[BF$_4$] is shown in *Figure 3*. The asymmetric unit contains two independent molecules with slightly different geometries (for details see *Figure S6* and *Table S2*). The complex adopts a distorted square planar coordination geometry at the Rh center with a metal-arene interaction to the C$_{ipso}$ of one of the aryl groups of the NHC ligand side arm (Rh1—C12$_{avg}$ = 2.486 Å) to stabilize the coordinatively unsaturated metal, in line with reported unsaturated rhodium NHC complexes (*Figure 2*). The Rh-carbene bond is tilted (Rh1—C9—N1$_{avg}$ = 103.2°, Rh1—C9$_{avg}$ = 2.030 Å), but not elongated compared to the chloride complex (Rh1—C9—N1 = 125.9(2)°, Rh1—C9 = 2.075(2) Å).[42] The bond lengths and angles to the COD ligand are not significantly changed from the chloride complex.

The change in steric influence due to the tilting was evaluated using buried volume analysis with

Figure 2. Coordinatively unsaturated tilted cationic and zwitterionic Rh(I) and Ir(I) NHC complexes.
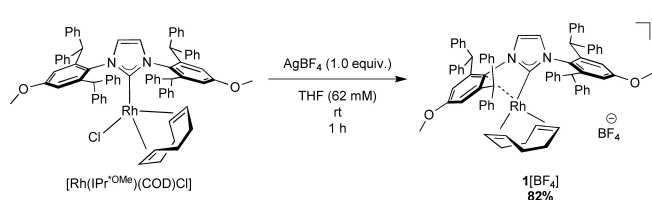
Scheme 1. Synthesis of complex **1**[BF$_4$] by chloride abstraction using Ag(I).
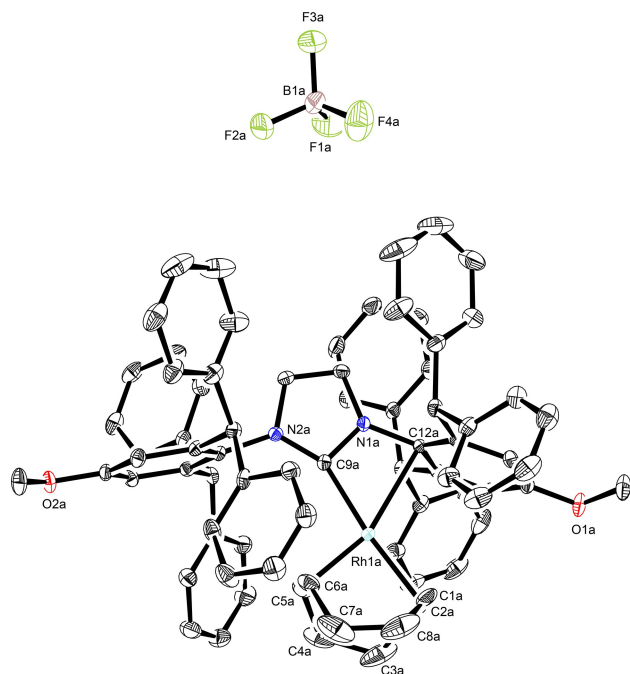
Figure 3. ORTEP diagram of **1**[BF$_4$] (only one of the two independent molecules is shown) with thermal ellipsoids at 50 % probability. Hydrogen atoms and solvent molecules are omitted for clarity. For bond lengths and angles of both molecules, see *Supporting Information*.

SambVca.[43] In complex **1**[BF$_4$] the ligand exhibits a buried volume of V$_{Bur}$ = 48.6 % (*Figure 4*), which is significantly higher than that in the parent chloride complex (V$_{Bur}$ = 37.2 %),[42] and the steric demand is more pronounced on the side with the metal-arene interaction.
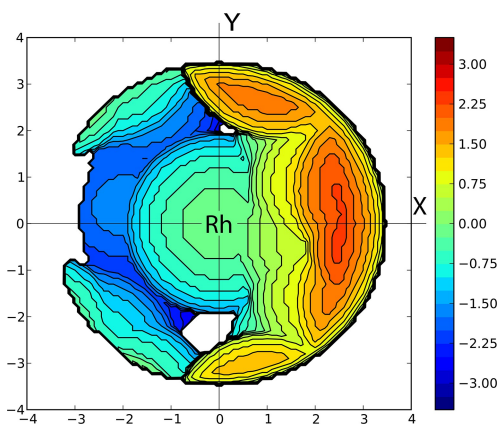

Figure 4. Buried volume analysis (3.5 Å radius) of **1** generated with SambVca.[43] The Z-axis is defined as the Rh-NHC axis. Calculation parameters: sphere radius, 3.50 Å; hydrogen atoms were omitted; *Bondi* radii scaled by 1.17.

In contrast to the tilted structure in the solid state, **1**[BF$_4$] is fluxional in the solution state on the NMR timescale at room temperature, as witnessed by the C$_2$ symmetry of the NHC ligand in the ^{1}H- and ^{13}C-NMR spectra. The two alkene signals of the COD ligand are inequivalent in the ^{1}H-NMR spectrum, however, and shifted upfield compared to the neutral chloride complex. In the ^{13}C-NMR spectrum one CH$_2$=CH$_2$ signal of the COD moiety is clearly resolved (72.1 ppm (*d*, *J* = 16.8 Hz)), while the other is broadened (103.3 ppm (br. *s*, $\nu_{1/2}$ = 52 Hz)), hinting at a dynamic behavior in solution. The carbene signal in **1**[BF$_4$] was not observed but is expected to become more shielded with an increase in tilting of the metal-NHC axis according to the literature.[35,36] The shift of the rhodium center was detected indirectly in a ^{1}H,^{103}Rh-HMBC experiment, and resonated at −7300 ppm, which is less shielded compared to the chloride analog (−7535 ppm).[42] The molecular symmetry indicated from the ^{1}H-NMR spectrum is retained down to −80 °C, indicating a low barrier for the dynamic behavior in solution (*Figures S1 – S2*).

Reactivity Towards Dihydrogen

We next wondered whether the COD ligand in cationic complex **1** could be hydrogenated to afford a well-defined coordinatively unsaturated rhodium species. To this end, a yellow suspension of **1**[BF$_4$] in THF-d_8 in a *J-Young* NMR tube was pressurized with 1 bar of hydrogen in the frozen state (*Scheme 2*). Within minutes at room temperature, the solid dissolved and the color of the resulting mixture turned light yellow.

The ^{1}H-NMR spectrum of the resulting clear yellow solution after 30 minutes at room temperature showed full conversion of **1**[BF$_4$] towards a major (red circles) and a minor species (blue squares) (*Figure 5*). The major species **2**[BF$_4$] features multiple broadened signals between 6.3 – 4.8 ppm and a lower symmetry at the NHC ligand. The upfield shift of the signals derived from the NHC ligand suggests coordination of an arene to rhodium. Furthermore, a characteristic metal-hydride signal at −12.14 ppm (2H, *d*, J_{Rh-H} =
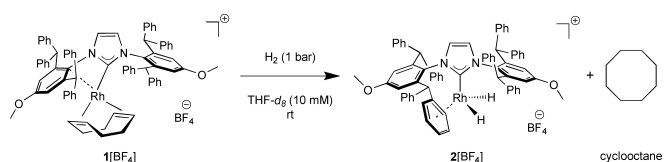
Scheme 2. Reaction of **1**[BF$_4$] with hydrogen to afford dihydride complex **2**[BF$_4$].
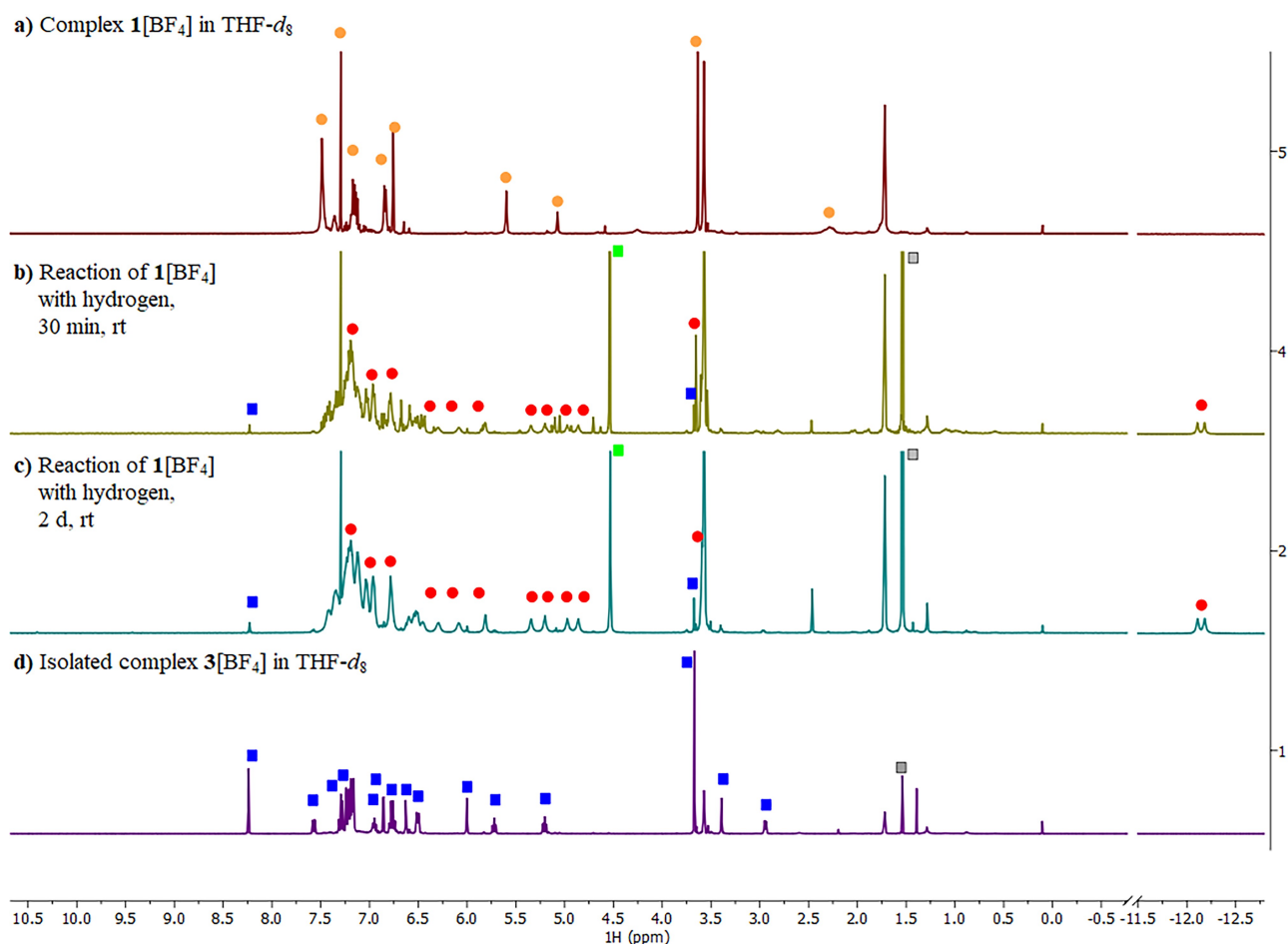
Figure 5. Stacked ^{1}H-NMR spectra of (a) isolated **1**[BF$_4$] in THF-d_8 (orange circles); (b) the mixture under dihydrogen atmosphere (green square) after 30 min; (c) after two days; (d) isolated **3**[BF$_4$] in THF-d_8. Two complexes are formed in the reaction, a rhodium-hydride complex (**2**[BF$_4$], red circles) and another hydride-free complex (**3**[BF$_4$], blue squares), as well as cyclooctane (grey square).

29.1 Hz) was detected indicating two chemically equivalent hydrides, alongside a *singlet* at 1.54 ppm corresponding to cyclooctane (grey square) resulting from COD hydrogenation. The cross-peak of the hydride signal in the ^{1}H,^{103}Rh-HMBC spectrum (−7253 ppm) unambiguously confirms the presence of a rhodium-bound hydride. The minor species (**3**[BF$_4$]) decreased over the course of the reaction but remained in small quantities. After two days under hydrogen atmosphere, a steady state between the dihydride complex **2** and species **3** was reached, while excess dihydrogen remained (*singlet* at 4.53 ppm, green square). In the ^{13}C{^{1}H}NMR spectrum the carbene signal was detected at 170.1 ppm (*d*, *J* = 62.1 Hz) which is shifted significantly upfield from the parent complex [Rh(IPr*^{OMe})(COD)Cl].

Notably, when the H$_2$ pressure was released, the color of the solution changed from light yellow to brown. The NMR spectrum of the isolated product after evaporation matches the intermediately formed minor species **3**[BF$_4$] (blue squares) detected *in situ*, suggesting that the proposed dihydride complex **2** is only stable under a hydrogen atmosphere.

To gain insight into the structure of dihydride complex **2**, we performed density functional theory (DFT) calculations (for computational details see *Supporting Information*). The bond lengths and angles of the DFT optimized structure of **1** were in good agreement with the X-ray structure (*Table S4*), benchmarking the DFT methodology to calculate the geometries of the complexes.

The optimized structure of dihydride complex **2** is shown in *Figure 6*. One of the peripheral phenyl groups of the NHC ligand coordinates to the metal center in an η^6 fashion, in accord with the NMR assignment. The two hydrides are in an equatorial position compared to the axial carbene ligand. The rhodium-hydride bond distances lie in the typical
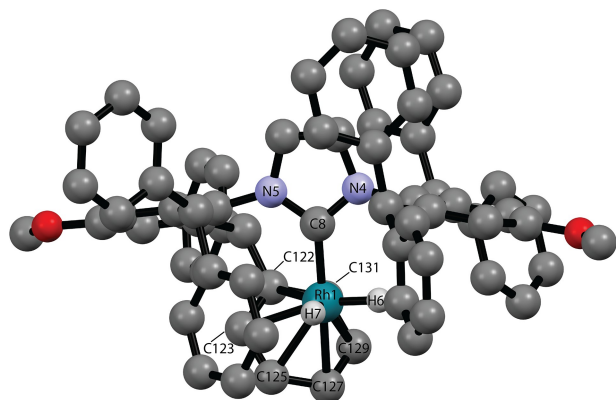
Figure 6. Calculated structure of **2**. Hydrogen atoms except hydrides are omitted for clarity. Selected bond lengths [Å] and angles [°]: Rh1–C8 1.961, Rh1–(C122,123,125,127,129,131) 2.299–2.369, Rh1–H6 1.532, Rh1–H7 1.535, H6–H7 1.772, H6–Rh1–H7 70.6, Rh1–C8–N4 129.9, Rh1–C8–N5 124.9.

range of Rh(III)-hydride complexes,[44] which leads to the assignment of a Rh(III) d^6 center with an 18 e$^−$ configuration. Complexes of the composition [M-(NHC)(H)$_2$(η^6-arene)]$^+$ (M=Rh, Ir) have been synthesized previously by hydrogenation of their corresponding cationic COD complexes in the presence of (fluorinated) arene solvents.[35,45] However, complex **2** is a rare example of a monomeric rhodium(III) NHC complex where the coordinated arene is a substituent on the NHC ligand in its coordination sphere. Notably, when the reaction was carried out in a mixture of THF/toluene (20:1), no coordination of toluene was observed by ^{1}H-NMR spectroscopy (*Figure S4*).

To isolate and characterize product **3**[BF$_4$] obtained after hydrogenation, the reaction was carried out on a preparative scale (0.155 mmol) in a 100 mL *J-Young* flask. A suspension of **1**[BF$_4$] in THF was stirred under 1 bar hydrogen atmosphere at ambient temperature for 24 hours. The resulting solution was evaporated *in vacuo* to directly afford complex **3**[BF$_4$] (*Scheme 3*).

Complex **3**[BF$_4$] was characterized by NMR spectroscopy. In contrast to **2**, complex **3** does not contain hydride ligands, according to the ^{1}H-NMR spectrum.
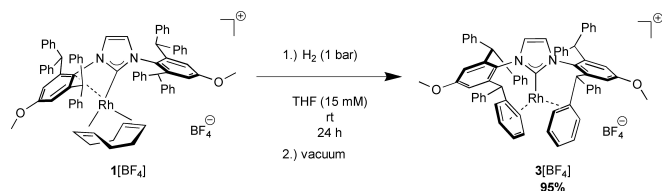

**Scheme 3.** Reaction of **1**[BF$_4$] with hydrogen, followed by evacuation to afford **3**[BF$_4$].

Several upfield-shifted multiplet signals down to 2.94 ppm again suggest an η^6-coordination mode of one of the aryl rings of the NHC ligand. Similarly, the ^{13}C-NMR spectrum features six doublets between 140–84 ppm, in line with the assignment of a coordinated arene ligand to a rhodium center (I=$\frac{1}{2}$). The carbene resonance was found at 166.8 ppm (*d*, *J*=63.7 Hz), slightly upfield to dihydride complex **2**. Moreover, the ^{1}H,^{103}Rh-HMBC spectrum shows two cross-peaks that stem from couplings of the metal to a coordinated aryl ring ($\delta(^{103}$Rh) = −7539 ppm, $\delta(^1$H) = 7.57, 2.94 ppm).

Our attempts to obtain a single crystal X-ray structure of **3**[BF$_4$] were unsuccessful. DFT studies were carried out to validate the proposed coordination chemistry of the complex. The optimized structure of **3** is shown in *Figure 7*. The rhodium center is coordinated by the carbene, and two π systems of the peripheral phenyl rings of the NHC ligand, in η^6 and in η^2 fashion, respectively. The buried volume of the ligand in this conformation is exceptionally high at 93.6% (*Figure 8*). This example represents a rare coordination mode wherein a Rh(I) complex is exclusively coordinated to an NHC ligand rather than an external arene.

Finally, we wondered whether H–H bond reductive elimination from **2** to form complex **3** is reversible. Subjecting a THF-d_8 solution of **3**[BF$_4$] to 1 bar hydrogen atmosphere resulted in the generation of dihydride complex **2**[BF$_4$] within 40 minutes (*Scheme 4*, *Figure S5*). After 18 hours no further conversion was observed in the presence of dihydrogen, which might indicate a hydrogen pressure-dependent equilibrium between **2** and **3**. Upon degassing the solution,
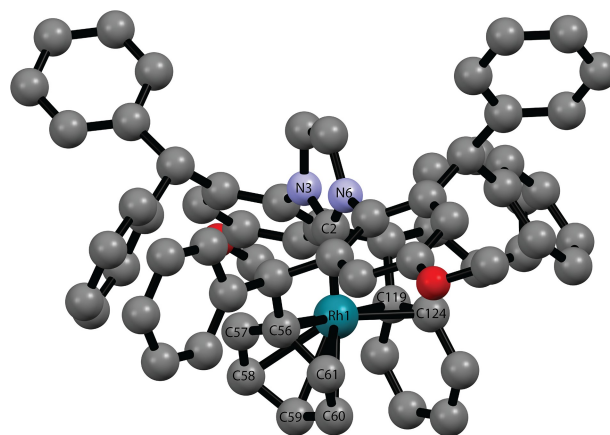
Figure 7. Calculated structure of **3**. Hydrogen atoms are omitted for clarity. Selected bond lengths [Å] and angles [°]: Rh1–C2 1.960, Rh1–(C56–61) 2.200–2.404, Rh1–(C119,124) 2.209–2.229, Rh1–C2–N3 127.0, Rh1–C2–N6 104.7.

HELVETICA
chimica acta
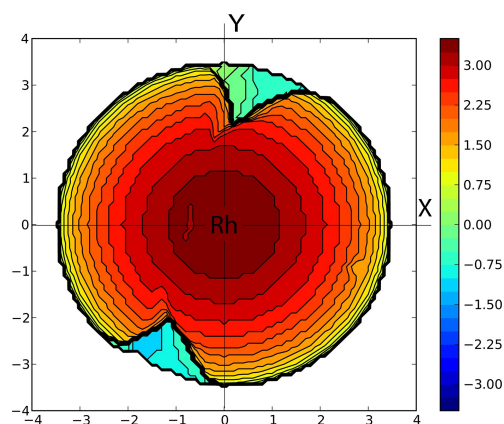
Figure 8. Buried volume analysis (3.5 Å radius) of **3** generated with SambVca.[43] The Z-axis is defined as the Rh–NHC axis. Calculation parameters: sphere radius, 3.50 Å; hydrogen atoms were omitted; *Bondi* radii scaled by 1.17.
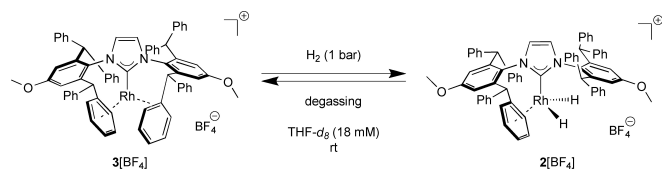
Scheme 4. Reversible addition of dihydrogen to complex **3**[BF$_4$].

complex **3** is regenerated within 30 minutes, clearly establishing the reversibility of oxidative addition of dihydrogen.

Conclusions

In summary, we reported the facile synthesis of some rhodium NHC complexes with an unusual coordination mode. [Rh(Ipr*^{OMe})(COD)]BF$_4$ exists in a tilted, pseudo-square planar coordination geometry, where an arene serves as an ancillary ligand, in line with reported cationic rhodium NHC complexes. This complex can be hydrogenated to form a transiently stable dihydride complex, which eliminates H$_2$ to release a cationic Rh(I) complex coordinated to a single NHC ligand.

With respect to the far-reaching applications of homogeneous rhodium complexes in hydrogenations, we expect that the well-defined highly unsaturated rhodium complexes disclosed herein may serve as both highly active precatalysts and as mechanistic tools to study new and established catalytic reactions.

Experimental Section

General Information

All air- and moisture-sensitive experiments were carried out either in a glovebox (*LABmaster Pro SP, Mbraun*) under an argon atmosphere or under a nitrogen atmosphere using standard *Schlenk* techniques. All glassware was stored in a pre-heated oven prior to use. Nitrogen was dried using a drying tube equipped with *Drierite™*. Diethyl ether, tetrahydrofuran (THF), THF-d_8, dichloromethane (CH$_2$Cl$_2$), CD$_2$Cl$_2$, and hexane were dried using the appropriate drying agents, degassed, distilled prior to use, and stored over molecular sieves. Gaseous dihydrogen ($\geq$ 99.999%) was purchased from *Pangas* and used as received. [Rh(Ipr*^{OMe})(COD)Cl] was synthesized according to a literature procedure.[42] Nuclear magnetic resonance (NMR) spectra were acquired on commercial instruments (*Bruker Avance III* 400 MHz, *Bruker Neo* 400 MHz, *Bruker Avance III* 500 MHz, all equipped with a BBFO probe) at the NMR facility of ETH Zürich. All spectra were acquired at 298 K unless stated otherwise. The proton signal of the residual non-deuterated solvent (δ 5.32 ppm for CD$_2$Cl$_2$, and δ 1.72 ppm for THF-d_8, resp.) was used as an internal reference for ^{1}H-NMR spectra. For ^{13}C{^{1}H}-NMR spectra, chemical shifts are reported relative to the solvent signal: δ 53.84 ppm for CD$_2$Cl$_2$, and δ 67.21 ppm for THF-d_8, respectively). ^{19}F{^{1}H}-NMR spectra are reported against an external standard, CFCl$_3$. ^{103}Rh signals were detected indirectly in a ^{1}H,^{103}Rh-HMBC experiment (pulse sequence: hmbcgpndqf). Coupling constants are reported in Hz. Multiplicities are indicated by s (singlet), d (doublet), t (triplet), q (quartet), sept (septet), m (multiplet), br. (broad) and combinations thereof. High-resolution mass spectra were provided by the mass spectrometry service facility in the Laboratories of Organic Chemistry at ETH Zürich. The molecular ion [M]$^+$ and [M + H]$^+$ are given in *m/z* units. ATR-FT-IR spectra were recorded in a glovebox under an argon atmosphere on a *Bruker ALPHA II* FT-IR spectrometer. The absorption bands are reported in cm^{-1} and are described as follows: strong (s), medium (m), weak (w), broad (br.), and shoulder (sh). The details for XRD studies are given in the *Supporting Information*.

[Rh(Ipr*^{OMe})(COD)]BF$_4$ (**1**[BF$_4$]). In a glovebox, a 50 mL Schlenk round bottom flask equipped with a magnetic stirring bar under argon was charged with [Rh(Ipr*^{OMe})(COD)Cl] (431.9 mg, 1.00 Eq, 343.0 µmol). Another 20 mL Schlenk tube was charged with AgBF$_4$ (70.1 mg, 1.05 Eq, 360.2 µmol) and shielded from light.

Both vessels were cycled onto the Schlenk line, and the solids were dissolved in THF (4.0 mL for rhodium complex; 1.0 mL for silver salt). The silver salt solution was added to the rhodium complex solution through cannula transfer. The residual was taken up and transferred with THF (0.5 mL). Upon adding the silver solution, the mixture turned orange and a precipitate formed. The mixture was stirred at ambient temperature for 1 hour, and then filtered through cannula into a new 50 mL Schlenk round bottom flask. The residual was washed with THF (1.5 mL). The obtained orange clear solution was concentrated to about 10% of the original volume. The concentrated solution was triturated with diethyl ether (8.0 mL). A yellow solid precipitated. The supernatant was cannula filtered into another new 50 mL Schlenk round bottom flask, and the solid was dried under high vacuum to afford the title compound (348.5 mg, 280.3 µmol, 82%) as an orange-yellow solid. Single crystals suitable for X-ray diffraction analysis were obtained by layering a CH_2Cl_2 solution with diethyl ether. ^{1}H-NMR (500 MHz, CD_2Cl_2): 7.50–7.44 (m, 16H), 7.44–7.39 (m, 4H), 7.21–7.16 (m, 12H), 6.81–6.76 (m, 8H), 6.72 (s, 4H), 5.51 (s, 4H), 4.90 (s, 2H), 4.36 (s, 2H), 3.65 (s, 6H), 3.24 (s, 2H), 2.40 (s, 2H), 2.30–2.17 (m, 2H), 1.85–1.68 (m, 4H). ^{13}C{^{1}H}-NMR (126 MHz, CD_2Cl_2): 162.1, 144.0, 142.5, 141.5, 130.2, 129.5, 129.1, 129.0, 128.7, 128.3, 127.9, 124.4, 115.8, 103.3 (br. S), 72.1 (d, *J* = 16.8), 103.3, 56.1, 53.2, 33.4, 27.1. The carbene signal was not observed, even with prolonged measuring time. ^{19}F{^{1}H}-NMR (471 MHz, CD_2Cl_2): −153.4. ^{11}B-NMR (160 MHz, CD_2Cl_2): −1.2. ^{103}Rh-NMR (16 MHz, CD_2Cl_2): −7300. IR (ATR) 3025 (w), 1590 (m), 1493 (w), 1465 (m), 1442 (m), 1302 (w), 1218 (w), 1145 (w), 1049 (s), 956 (w), 857 (w), 766 (w), 699 (s), 648 (w), 622 (w), 603 (m), 580 (w), 519 (w), 478 (w), 456 (w). HR-MS: 1155.4301 ($C_{77}H_{68}N_2O_2Rh^+$, M^+; calc. 1155.4330). CCDC-2226562 contains the crystallographic data.

[Rh(IPr*^{OMe})]BF$_4$ (**3**[BF$_4$]). In a glovebox, a 100 mL *J-Young* Schlenk tube was charged with **1**[BF$_4$] (192.4 mg, 1.00 Eq, 154.8 µmol) and THF (10.0 mL), and stirred for several minutes to give a yellow suspension (partially dissolved). The mixture was frozen with liquid nitrogen and the headspace was evacuated. The reaction was then pressurized with hydrogen (1.0 bar) in the frozen state, sealed, and allowed to thaw. The mixture was stirred for 24 h at ambient temperature under hydrogen atmosphere. Within 30 minutes, a clear brown solution formed, which discolored over time. At the end of the reaction, a clear yellow solution resulted. The pressure was vented to the Schlenk line,

and the mixture was evaporated. Upon concentration, the color changed gradually to orange and brown. The dry residue was transferred into a glovebox and triturated with hexane (5 mL). The resulting solid was washed with hexane (2×3 mL) and dried to afford the title compound (166.1 mg, 146.4 µmol, 95%) as a brown solid. Trace amounts of cyclooctane could not be removed after prolonged drying under high vacuum, in line with previous observations with nickel arene complexes.[46] ^{1}H-NMR (500 MHz, THF-d_8): 8.25 (s, 2H), 7.57 (br. D, *J* = 7.8, 2H), 7.32–7.14 (m, 20H), 6.97–6.93 (m, 2H), 6.86 (d, *J* = 2.9, 2H), 6.80–6.72 (m, 6H), 6.63 (d, *J* = 2.9, 2H), 6.52–6.49 (m, 4H), 6.01 (s, 2H), 5.72 (ddd, *J* = 7.8, 6.6, 1.2, 2H), 5.21 (td, *J* = 7.0, 1.1, 2H), 3.67 (s, 6H), 3.39 (s, 2H), 2.94 (br. Dt, *J* = 6.4, 1.3, 2H). ^{13}C{^{1}H}-NMR (126 MHz, THF-d_8): 166.6 (d, *J* = 63.7), 160.0, 144.1, 142.1, 141.8 (d, *J* = 3.6), 141.6, 131.3, 130.0, 129.9 (d, *J* = 6.6), 129.6, 129.1, 128.8, 128.0 (d, *J* = 13.0), 127.3 (d, *J* = 25.0), 124.6, 122.1, 121.1, 119.5, 117.2, 114.7, 98.6 (d, *J* = 7.6), 84.0 (d, *J* = 6.2), 55.5, 53.3, 51.9. ^{19}F{^{1}H}-NMR (377 MHz, THF-d_8): −152.5. ^{11}B-NMR (128 MHz, THF-d_8): −0.9. ^{103}Rh-NMR (16 MHz, THF-d_8): −7539. IR (ATR) 2931 (w), 1598 (m), 1494 (m), 1468 (m), 1446 (sh), 1314 (w), 1215 (w), 1147 (sh), 1049 (m), 856 (w), 755 (m), 699 (s), 617 (w), 597 (m), 518 (w), 449 (w). HR-MS: 1047.3422 ($C_{69}H_{56}N_2O_2Rh^+$, M^+; calc. 1047.3391).

Supplementary Material

Synthetic protocols and characterization of the new compounds are reported in the electronic supporting information. Supporting information for this article is available on the WWW under https://doi.org/10.1002/hlca.202200199.

CCDC deposition number 2226562 contains the supplementary crystallographic data for this paper. These data are provided free of charge by the Cambridge Crystallographic Data Centre.

Acknowledgements

HELVETICA
chimica acta

Data Availability Statement

The data that support the findings of this study are available from the corresponding author upon reasonable request.

Author Contribution Statement

M. L. and H. Z. conceived the study, designed and performed the experiments, and analyzed the data. N. T. carried out the X-ray crystallographic analysis. B. M. supervised the work. M. L., H. Z. and B. M. wrote the manuscript.

References

[1] D. S. Surry, S. L. Buchwald, 'Biaryl Phosphane Ligands in Palladium-Catalyzed Amination', *Angew. Chem. Int. Ed.* **2008**, *47*, 6338–6361.

[2] T. E. Barder, S. D. Walker, J. R. Martinelli, S. L. Buchwald, 'Catalysts for Suzuki–Miyaura Coupling Processes: Scope and Studies of the Effect of Ligand Structure', *J. Am. Chem. Soc.* **2005**, *127*, 4685–4696.

[3] C.-S. Li, C.-H. Cheng, F.-L. Liao, S.-L. Wang, 'Insertion of norbornadiene into the aryl-palladium bond; synthesis, structure and dynamics of intramolecular η^2-arene palladium species', *J. Chem. Soc. Chem. Commun.* **1991**, 710–712.

[4] D. I. Chai, P. Thansandote, M. Lautens, 'Mechanistic Studies of Pd-Catalyzed Regioselective Aryl C–H Bond Functionalization with Strained Alkenes: Origin of Regioselectivity', *Chem. Eur. J.* **2011**, *17*, 8175–8188.

[5] E. A. B. Kantchev, C. J. O'Brien, M. G. Organ, 'Palladium Complexes of N-Heterocyclic Carbenes as Catalysts for Cross-Coupling Reactions – A Synthetic Chemist's Perspective', *Angew. Chem. Int. Ed.* **2007**, *46*, 2768–2813.

[6] S. Díez-González, N. Marion, S. P. Nolan, 'N-Heterocyclic Carbenes in Late Transition Metal Catalysis', *Chem. Rev.* **2009**, *109*, 3612–3676.

[7] G. C. Vougioukalakis, R. H. Grubbs, 'Ruthenium-Based Heterocyclic Carbene-Coordinated Olefin Metathesis Catalysts', *Chem. Rev.* **2010**, *110*, 1746–1787.

[8] G. C. Fortman, S. P. Nolan, '*N*-Heterocyclic carbene (NHC) ligands and palladium in homogeneous cross-coupling catalysis: a perfect union', *Chem. Soc. Rev.* **2011**, *40*, 5151–5169.

[9] C. S. J. Cazin, 'N-Heterocyclic Carbenes in Transition Metal Catalysis and Organocatalysis', Springer, Dordrecht, 2011.

[10] M. Soleilhavoup, G. Bertrand, 'Cyclic (Alkyl)(Amino)Carbenes (CAACs): Stable Carbenes on the Rise', *Acc. Chem. Res.* **2015**, *48*, 256–266.

[11] S. P. Nolan, C. S. J. Cazin, 'N-Heterocyclic Carbenes in Catalytic Organic Synthesis', in 'Science of Synthesis', Thieme, Stuttgart, Germany, 2017.

[12] C. Valente, S. Çalimsiz, K. H. Hoi, D. Mallik, M. Sayah, M. G. Organ, 'The Development of Bulky Palladium NHC Complexes for the Most-Challenging Cross-Coupling Reactions', *Angew. Chem. Int. Ed.* **2012**, *51*, 3314–3332.

[13] S. Meiries, K. Speck, D. B. Cordes, A. M. Z. Slawin, S. P. Nolan, '[Pd(Ipr*^{OMe})(acac)Cl]: Tuning the N-Heterocyclic Carbene in Catalytic C–N Bond Formation', *Organometallics* **2013**, *32*, 330–339.

[14] C. Valente, M. Pompeo, M. Sayah, M. G. Organ, 'Carbon-Heteroatom Coupling Using Pd-PEPPSI Complexes', *Org. Process Res. Dev.* **2014**, *18*, 180–190.

[15] S. M. P. Vanden Broeck, F. Nahra, C. S. J. Cazin, 'Bulky-Yet-Flexible Carbene Ligands and Their Use in Palladium Cross-Coupling', *Inorganics* **2019**, *7*, 78.

[16] Y. Xia, G. Lu, P. Liu, G. Dong, 'Catalytic activation of carbon-carbon bonds in cyclopentanones', *Nature* **2016**, *539*, 546–550.

[17] Y. Xia, G. Dong, 'Temporary or removable directing groups enable activation of unstrained C–C bonds', *Nat. Rev. Chem.* **2020**, *4*, 600–614.

[18] L. Deng, G. Dong, 'Carbon-Carbon Bond Activation of Ketones', *Trends Chem.* **2020**, *2*, 183–198.

[19] M. D. R. Lutz, B. Morandi, 'Metal-Catalyzed Carbon-Carbon Bond Cleavage of Unstrained Alcohols', *Chem. Rev.* **2021**, *121*, 300–326.

[20] Y. Wei, B. Rao, X. Cong, X. Zeng, 'Highly Selective Hydrogenation of Aromatic Ketones and Phenols Enabled by Cyclic (Amino)(alkyl)carbene Rhodium Complexes', *J. Am. Chem. Soc.* **2015**, *137*, 9250–9253.

[21] M. P. Wiesenfeldt, Z. Nairoukh, W. Li, F. Glorius, 'Hydrogenation of fluoroarenes: Direct access to all-*cis*-(multi)fluorinated cycloalkanes', *Science* **2017**, *357*, 908–912.

[22] B. L. Tran, J. L. Fulton, J. C. Linehan, J. A. Lercher, R. M. Bullock, 'Rh(CAAC)-Catalyzed Arene Hydrogenation: Evidence for Nanocatalysis and Sterically Controlled Site-Selective Hydrogenation', *ACS Catal.* **2018**, *8*, 8441–8449.

[23] M. P. Wiesenfeldt, Z. Nairoukh, T. Dalton, F. Glorius, 'Selective Arene Hydrogenation for Direct Access to Saturated Carbo- and Heterocycles', *Angew. Chem. Int. Ed.* **2019**, *58*, 10460–10476.

[24] J. Lee, H. Hahm, J. Kwak, M. Kim, 'New Aspects of Recently Developed Rhodium(N-Heterocyclic Carbene)-Catalyzed Organic Transformations', *Adv. Synth. Catal.* **2019**, *361*, 1479–1499.

[25] Z. Nairoukh, M. Wollenburg, C. Schlepphorst, K. Bergander, F. Glorius, 'The formation of all-*cis*-(multi)fluorinated piperidines by a dearomatization-hydrogenation process', *Nat. Chem.* **2019**, *11*, 264–270.

[26] D. Moock, M. P. Wiesenfeldt, M. Freitag, S. Muratsugu, S. Ikemoto, R. Knitsch, J. Schneidewind, W. Baumann, A. H. Schäfer, A. Timmer, M. Tada, M. R. Hansen, F. Glorius, 'Mechanistic Understanding of the Heterogeneous, Rho-

dium-Cyclic (Alkyl)(Amino)Carbene-Catalyzed (Fluoro-)Arene Hydrogenation', *ACS Catal.* **2020**, *10*, 6309–6317.

[27] R. R. Schrock, J. A. Osborn, 'Catalytic Hydrogenation Using Cationic Rhodium Complexes. I. Evolution of the Catalytic System and the Hydrogenation of Olefins', *J. Am. Chem. Soc.* **1976**, *98*, 2134–2143.

[28] R. R. Schrock, J. A. Osborn, 'Catalytic Hydrogenation Using Cationic Rhodium Complexes. II. The Selective Hydrogenation of Alkynes to Cis Olefins', *J. Am. Chem. Soc.* **1976**, *98*, 2143–2147.

[29] R. R. Schrock, J. A. Osborn, 'Catalytic Hydrogenation Using Cationic Rhodium Complexes. 3. The Selective Hydrogenation of Dienes to Monoenes', *J. Am. Chem. Soc.* **1976**, *98*, 4450–4455.

[30] A. C. Hillier, H. M. Lee, E. D. Stevens, S. P. Nolan, 'Cationic Iridium Complexes Bearing Imidazol-2-ylidene Ligands as Transfer Hydrogenation Catalysts', *Organometallics* **2001**, *20*, 4246–4252.

[31] L. D. Vazquez-Serrano, B. T. Owens, J. M. Buriak, 'The search for new hydrogenation catalyst motifs based on N-heterocyclic carbene ligands', *Inorg. Chim. Acta* **2006**, *359*, 2786–2797.

[32] Y. Zhang, D. Wang, K. Wurst, M. R. Buchmeiser, 'Polymerization of phenylacetylene by novel Rh (I)-, Ir (I)- and Ru (IV) 1,3-R$_2$-3,4,5,6-tetrahydropyrimidin-2-ylidenes (R = mesityl, 2-propyl): Influence of structure on activity and polymer structure', *J. Organomet. Chem.* **2005**, *690*, 5728–5735.

[33] N. Stylianides, A. A. Danopoulos, N. Tsoureas, 'Pyridine and phosphine functionalised *N*-heterocyclic carbene complexes of rhodium and iridium', *J. Organomet. Chem.* **2005**, *690*, 5948–5958.

[34] V. César, N. Lugan, G. Lavigne, 'Electronic Tuning of a Carbene Center via Remote Chemical Induction, and Relevant Effects in Catalysis', *Chem. Eur. J.* **2010**, *16*, 11432–11442.

[35] E. L. Kolychev, S. Kronig, K. Brandhorst, M. Freytag, P. G. Jones, M. Tamm, 'Iridium(I) Complexes with Anionic N-Heterocyclic Carbene Ligands as Catalysts for the Hydrogenation of Alkenes in Nonpolar Media', *J. Am. Chem. Soc.* **2013**, *135*, 12448–12459.

[36] G. Sipos, A. Ou, B. W. Skelton, L. Falivene, L. Cavallo, R. Dorta, 'Unusual NHC-Iridium(I) Complexes and Their Use in the Intramolecular Hydroamination of Unactivated Aminoalkenes', *Chem. Eur. J.* **2016**, *22*, 6939–6946.

[37] P. Gao, G. Sipos, D. Foster, R. Dorta, 'Developing NHC-Iridium Catalysts for the Highly Efficient Enantioselective Intramolecular Hydroamination Reaction', *ACS Catal.* **2017**, *7*, 6060–6064.

[38] G. Sipos, P. Gao, D. Foster, B. W. Skelton, A. N. Sobolev, R. Dorta, 'In-Depth Study on Chloride Abstractions from (NHC)Ir(COD)Cl Complexes', *Organometallics* **2017**, *36*, 801–817.

[39] P. Gao, D. Foster, G. Sipos, B. W. Skelton, A. N. Sobolev, R. Dorta, 'Chiral NHC-Iridium Complexes and Their Performance in Enantioselective Intramolecular Hydroamination and Ring-Opening Amination Reactions', *Organometallics* **2020**, *39*, 556–573.

[40] L. P. Ho, A. Neitzel, T. Bannenberg, M. Tamm, 'Rhodium and Iridium Complexes of Anionic Thione and Selone Ligands Derived from Anionic N-Heterocyclic Carbenes', *Chem. Eur. J.* **2022**, *28*, e202104139.

[41] R. H. Crabtree, 'Resolving Heterogeneity Problems and Impurity Artifacts in Operationally Homogeneous Transition Metal Catalysts', *Chem. Rev.* **2012**, *112*, 1536–1554.

[42] M. D. R. Lutz, V. C. M. Gasser, B. Morandi, 'Shuttle arylation by Rh(I) catalyzed reversible carbon-carbon bond activation of unstrained alcohols', *Chem* **2021**, *7*, 1108–1119.

[43] L. Falivene, Z. Cao, A. Petta, L. Serra, A. Poater, R. Oliva, V. Scarano, L. Cavallo, 'Towards the online computer-aided design of catalytic pockets', *Nat. Chem.* **2019**, *11*, 872–879.

[44] A. Bakac, 'Aqueous rhodium(III) hydrides and mononuclear rhodium(II) complexes', *Dalton Trans.* **2006**, *60*, 1589–1596.

[45] C. Y. Tang, J. Lednik, D. Vidovic, A. L. Thompson, S. Aldridge, 'Responses to unsaturation in iridium mono(*N*-heterocyclic carbene) complexes: synthesis and oligomerization of [LIr(H)$_2$Cl] and [LIr(H)$_2$]$^+$', *Chem. Commun.* **2011**, *47*, 2523–2525.

[46] Y. Hoshimoto, Y. Hayashi, H. Suzuki, M. Ohashi, S. Ogoshi, 'One-Pot, Single-Step, and Gram-Scale Synthesis of Mononuclear [(η^6-arene)Ni(N-heterocyclic carbene)] Complexes: Useful Precursors of the Ni^0-NHC Unit', *Organometallics* **2014**, *33*, 1276–1282.